



LETTER • **OPEN ACCESS**

Unexpected high contribution of in-cloud wet scavenging to nitrogen deposition induced by pumping effect of typhoon landfall in China

To cite this article: Qixin Tan *et al* 2023 *Environ. Res. Commun.* **5** 021005

View the [article online](#) for updates and enhancements.

You may also like

- [Typhoon enhancement of N and P release from litter and changes in the litter N:P ratio in a subtropical tidal wetland](#)
Weiqi Wang, Jordi Sardans, Chuan Tong et al.
- [Estimation of the damage area due to tropical cyclones using fragility curves for paddy rice in Japan](#)
Y Masutomi, T Iizumi, K Takahashi et al.
- [Risk-based versus storyline approaches for global warming impact assessment on basin-averaged extreme rainfall: a case study for Typhoon Hagibis in eastern Japan](#)
Tomohiro Tanaka, Hiroaki Kawase, Yukiko Imada et al.

Environmental Research Communications



LETTER

Unexpected high contribution of in-cloud wet scavenging to nitrogen deposition induced by pumping effect of typhoon landfall in China

OPEN ACCESS

RECEIVED

15 August 2022

REVISED

25 December 2022

ACCEPTED FOR PUBLICATION

3 February 2023



PUBLISHED

16 February 2023

Original content from this work may be used under the terms of the [Creative Commons Attribution 4.0 licence](#).

Any further distribution of this work must maintain attribution to the author(s) and the title of the work, journal citation and DOI.



Qixin Tan^{1,2} , Baozhu Ge^{1,*}, Syuichi Itahashi³ , Lu Gan⁴, Ying Zhang¹, Shuyan Xie⁵, Ying Liu⁶, Danhui Xu⁷, Xueshun Chen¹, Lin Wu¹, Xiaole Pan¹, Wei Wang⁸, Jianbin Wu⁹, Jie Li¹, Junhua Wang^{1,2}, Xiaobin Xu¹⁰, Joshua S Fu¹¹  and Zifa Wang^{1,2}

¹ State Key Laboratory of Atmospheric Boundary Layer Physics and Atmospheric Chemistry, Institute of Atmospheric Physics, Chinese Academy of Sciences, Beijing 100029, People's Republic of China

² University of Chinese Academy of Sciences, Beijing, 100049, People's Republic of China

³ Sustainable System Research Laboratory, Central Research Institute of Electric Power Industry (CRIEPI), Abiko, Chiba 270–1194, Japan

⁴ Beijing Weather Forecast Center, Beijing, 100089, People's Republic of China

⁵ State Environmental Protection Key Laboratory of Quality Control in Environmental Monitoring, China National Environmental Monitoring Centre, Beijing 100012, People's Republic of China

⁶ Laboratory for Climate Studies & CMA-NJU Joint Laboratory for Climate Prediction Studies, National Climate Center, China Meteorological Administration, Beijing, People's Republic of China

⁷ National Center for Climate Change Strategy and International Cooperation, Ministry of Ecology and Environment, Beijing 100035, People's Republic of China

⁸ National center for environmental quality forecast, CNEMC, 100012, Beijing, People's Republic of China

⁹ Clear Technology Co. Ltd, Beijing 100029, People's Republic of China

¹⁰ Key Laboratory for Atmospheric Chemistry, Chinese Academy of Meteorological Sciences, Beijing, People's Republic of China

¹¹ Department of Civil and Environmental Engineering, University of Tennessee, Knoxville, TN 37996, United States of America

* Author to whom any correspondence should be addressed.

E-mail: gebz@mail.iap.ac.cn

Keywords: in-cloud scavenging, wet deposition, source-receptor relationship, typhoon

Supplementary material for this article is available [online](#)

Abstract

Atmospheric nitrogen deposition has large eco-environmental effects such as ocean acidification, eutrophication in coastal areas. However, knowledge of the source and the pathway of N deposition in coastal areas is limited, especially during tropical storms, hindering the accurate quantification of how anthropogenic activities influence the ocean ecosystem. In this study, the Nested Air Quality Prediction Modeling System was used to investigate the wet deposition of N induced by typhoon Hagupit over eastern coastal China from an in- and below-cloud process perspective. Our results reveal for the first time an enhancement mechanism of N deposition related to the 'pumping effect' of the typhoon. Different from the non-typhoon conditions, air pollutants in the typhoon-affected regions were pumped into the higher altitudes and deposited via the in-cloud scavenging process in the moving path of the typhoon-affected regions. This study updates our understanding of the source–receptor relationship on atmospheric wet deposition caused by tropical cyclones.

1. Introduction

Atmospheric nitrogen (N) deposition has important eco-environmental effects, including acid rain (Page *et al* 2008, Du 2018), corrosion of buildings (Knotkova and Barton 1992), ocean acidification (Doney *et al* 2007), nutrient anomalies (Hao *et al* 2011) and biodiversity reduction (Pitcairn *et al* 2003). The economic development in the country around the Chinese inland sea and North Pacific Ocean has resulted in gradually increasing level of the nutrient concentration such as dissolved inorganic nitrogen (DIN), turning these oceanic regions into nitrogen-rich basins. Statistically, atmospheric N deposition has been proven to be a larger contributor to the DIN input into the ocean than the riverine input, providing 10%–40% of the N in N-limited coastal regions (Okin *et al* 2011, J Zhang *et al* 1999). Wang *et al* (2019) estimated that about 25.81% of the total DIN input in the

Yellow Sea and Bohai Sea derives from the atmospheric N deposition. The contribution of N deposition from China reported by Ge *et al* (2014) and Kajino *et al* (2013) is about 40%–60% and 51%–76%.

Typhoons usually carry associated hazards, such as strong winds, storm surges, and rainfall, which can cause considerable damage and disruption. In addition to these direct forms of damage, the wet deposition of nitrogen caused by typhoons, which also serves as a larger contributor of DIN, has also drawn much attention in coastal regions (Lin *et al* 2000, Sakihama and Tokuyama 2005, Fang *et al* 2009, Chen *et al* 2015, Toyonaga and Zhang 2016, Yan *et al* 2016, Tan *et al* 2018), especially against the background of global climate change, which has resulted in an increased frequency and intensity of typhoons over the past two decades (Webster *et al* 2006, Bender *et al* 2010, Knutson *et al* 2010). Lin *et al* (2000) reported that wet deposition caused by typhoons represented 20% of the total deposition based on three years of observations in a subtropical rainforest in Taiwan. Toyonaga and Zhang (2016) conducted continuous field measurements of wet deposition fluxes of ions at a coastal site in Japan from 1996 to 2003 and estimated an N wet deposition flux rate associated with typhoons of $1 \text{ meq m}^{-2} \text{ yr}^{-1}$. To a certain extent, these studies help us to understand the wet deposition of N caused by typhoons.

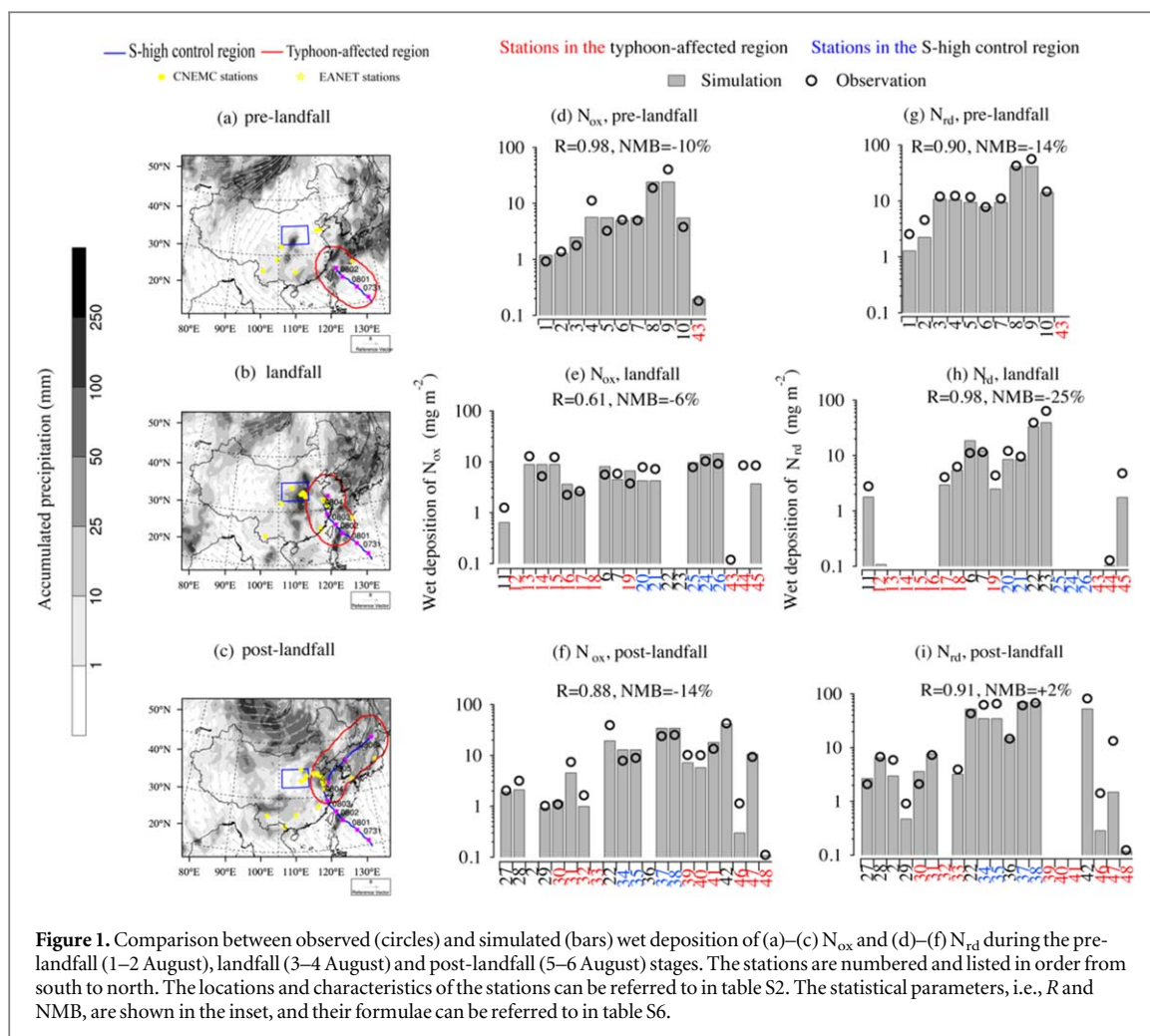
As we know, the wet deposition is governed by two main processes: in-cloud scavenging and below-cloud scavenging (Santachiara *et al* 2012, Ge *et al* 2014, Seinfeld and Pandis 2016, Xu *et al* 2017, 2019). For strong convective system (cold vortexes/typhoon), in-cloud contributions of inorganic nitrogen (IN) wet deposition are higher than thought, achieving 82% during continuous observations from 2013 to 2017 (Ge *et al* 2021). This reveals that the study on the source-receptor (S/R) of IN wet deposition during the typhoons should focus on the source of in-cloud IN wet deposition. However, knowledge of the source and pathway of N deposition by model simulation in coastal areas remains limited. Previous studies on the S/R relationship of deposition (Holloway *et al* 2002, Lin *et al* 2008, Kajino *et al* 2011, Kajino *et al* 2013), as well as multi-model comparisons (e.g., MICS-Asia III, HTAP II) (Tan *et al* 2018, Ge *et al* 2020), were able to quantitatively investigate the source of total wet deposition via sensitivity experiments but not in-cloud wet deposition. The sensitivity experiments to obtain the S/R of deposition inevitably introduce nonlinear errors caused by the changes in emission sources (Grewe 2004). Besides, these S/R relationship of IN deposition during non-typhoon period could not be applicable to that during typhoon due to different air conditions caused by typhoon (Chiang *et al* 2005, Fang *et al* 2009). This indicates the S/R relationships of N wet deposition during deep convective process of the typhoon, especially the source and pathway of N deposition should be explored to help us to improve the knowledge of the new mechanism of typhoon induced wet deposition.

In this study, we carried out simulations of the wet deposition of inorganic N (IN) during typhoon Hagupit (3–6 August 2020) induced by in- and below-cloud scavenging using the Nested Air Quality Prediction Modeling System (NAQPMS) (Wang *et al* 2001) coupled with the online tracer tagging method. Based on the simulation results, the influence of the typhoon on the wet deposition of IN, especially the in-cloud wet deposition in eastern China, is discussed. Besides, the source contributions of the in- and below-cloud wet deposition with the movement of the typhoon after it made landfall in the Yangtze River Delta (YRD) were quantified. The purpose of this study is to update our knowledge on the S/R relationships of in- and below-cloud wet deposition in typhoon-affected regions and explore the new mechanism of influence of typhoons on wet deposition.

2. Materials and methods

2.1. Model description and setup

NAQPMS is a 3D Eulerian terrain-following air quality model, which is developed by Wang *et al* (2001). It has been widely used to simulate the air pollutants, such as ozone (Li *et al* 2011, 2016), dust (Tian *et al* 2020), anthropogenic aerosols (Chen *et al* 2017, Wang *et al* 2017, Yang *et al* 2018, Du *et al* 2019), and even toxic pollutants like Mercury (Chen *et al* 2015), as well as the sulfur and nitrogen wet depositions over China (Ge *et al* 2014). Recently, NAQPMS has been invited to participate in the Model Inter-Comparison Study for Asia III (MICS-Asia III) to compare the simulated air pollutants (Li *et al* 2019, Kong *et al* 2020) as well as the depositions (Ge *et al* 2020, Itahashi *et al* 2020) over East Asia among 14 regional and global air quality models. In this study, the cloud processes schemes for in-cloud scavenging (Dennis *et al* 1993, Ge *et al* 2014) and the below-cloud scavenging scheme (Xu *et al* 2017, 2019, 2020) have been updated in NAQPMS to better simulate the wet deposition of air pollutants. In order to investigate the S/R of wet deposition of IN, an online tracer tagging module is also implemented in NAQPMS to track the formation and evolution of air pollutants (Li *et al* 2008, Wu *et al* 2017). Unlike other studies that can only track the source of the total wet deposition (Lin *et al* 2008, Kajino *et al* 2013), NAQPMS coupled with the on-line tracer tagging module can quantitatively estimate the S/R of the below- and in-cloud wet deposition without introducing errors by nonlinear chemistry. Further technical details about the NAQPMS can be found in Text S1–S2 and in Li *et al*, (2011;2013;2016) and Ge *et al* (2014).



The model domain covers the East Asia ($15.4^{\circ}S$ – $58.3^{\circ}N$, 48.5° – $160.2^{\circ}E$), which is set on a Lambert conformal map projection with 180×170 grids at 45 km horizontal resolution. Vertically, the numerical model has 20 terrain-following layers from the surface to the height of 20 km with the lowest 10 layers below 3 km. The global atmospheric chemical transport model MOZART v2.4 provided initial and lateral boundary conditions for the NAQPMs. The meteorological fields for NAQPMs were provided by the Weather Research and Forecasting (WRF) model, version 3.4.1 (Skamarock *et al* 2008) driven by National Centers for Environmental Prediction Final Analysis reanalysis data ($1^{\circ} \times 1^{\circ}$). More detailed descriptions of the WRF model including the Physics schemes can refer to in Text S3 and in Ge *et al* (2021). Emissions for NAQPMs are obtained from the emissions inventory in MICS-Asia III (Li *et al* 2017), and considering the yearly projections of the variations through the satellite-constrained NO_x and ammonia (NH_3) emissions based on vertical column density (VCD) values in 2020. More detailed descriptions of the updated emission can be found in Text S4. The model's output of IN wet deposition can be classified as oxidized N (N_{ox}), including particulate nitrate, gaseous nitrate acid and NO_x , and reduced N (N_{rd}) including NH_3 and particulate ammonium. The simulation period was from 24 July to 6 August 2020, with 8 days of model spin-up time from 24 to 31 July 2020.

Figure S1 shows 22 identified areas (ID) in the NAQPMs model simulation domain. Fifteen land areas in the territory of China (i.e., YRD, FJ, SD, NCP, SX, HN, AH, HB, JX, SW, TW, West, Middle, NW, and NE) are marked in different colors, together with North Korea (NK), South Korea (SK) and Japan. The three major oceanic regions along the pathway of typhoon Hagupit (green line depicted in figure S1) are marked as ECS (East China Sea), WP (West Pacific), and JS (Japan Sea), respectively. The definitions of the 22 IDs are listed in table S1.

2.2. Observational data

Ground-based observations of wet deposition collected at sites shown in figures 1(a)–(c) during 1–6 August 2020 by the China National Environmental Monitoring Centre (CNEMC) (<http://www.cnemc.cn>) and Acid Deposition Monitoring Network in East Asia (EANET) (<http://www.eanet.asia/>, last access date: 25 June 2022) were used to validate the performance of the model with respect to the wet deposition of N_{ox} and N_{rd} . Six of 48 stations are in SW, 9 in HN, 8 in SD, 11 in YRD, 4 in West, 4 in FJ, 2 in Middle, 1 in WP, 2 in Japan and 1 in

SX (table S2). The CNEMC observations of wet deposition included daily average inorganic ion concentrations (SO_4^{2-} , NO_3^- , NH_4^+ , F^- , Cl^- , Ca^{2+} , Mg^{2+} , Na^+ , and K^+) and daily accumulated precipitation from 1 to 6 August 2020. Because CNEMC sites mainly covered inland China, EANET sites located in coastal area over East Asia is additionally analyzed in this study (More information about the EANET observation can refer to Ge *et al* (2020)). After quality control (Text S5), the measured anion and cation concentrations of precipitation samples from 48 stations were nearly in balance and there were no large deficiencies of major inorganic ions. Surface observations of hourly $\text{PM}_{2.5}$ and NO_2 concentrations at the 48 stations from 1–6 August 2020 were also used in this study. Ground meteorological observations of daily precipitation and wind were obtained from China Meteorological Administration. The best-track data of typhoon Hagupit provided by the Japan Meteorological Agency were used to identify the location of the typhoon (<https://www.jma.go.jp/jma/jma-eng/jma-center/rsmc-hp-pub-e.g./besttrack.html>, last access: 16 December 2021).

2.3. Model validation

The NAQPMS was able to simulate the precipitation and wet deposition of IN both in typhoon-affected regions and in the other regions of China. The simulated accumulated precipitation in the typhoon-affected region during the pre-landfall (1–2 August), landfall (3–4 August), and post-landfall (5–6 August) stages shows good correlation, with a correlation coefficient (R) of 0.79 ($N = 11$), 0.78 ($N = 110$) and 0.75 ($N = 92$), and normalized mean bias (NMB) of -19% , -12.6% and 12.7% , respectively (figures 1(d)–(f)). In the S-high control region, the R values are 0.66 ($N = 48$), 0.64 ($N = 41$) and 0.68 ($N = 45$) for the pre-landfall, landfall and post-landfall stages, respectively, and the NMB values are -19.5% , 17.6% and -9.1% (figures S2(a), (b)). Compared to the reported statistical scores in MICS-Asia III (Ge *et al* 2020, Itahashi *et al* 2020), our modeling performance in this study have been confirmed as better. In accordance with the good model performance for precipitation, the simulated wet deposition of IN agrees well with the observations, with the NMB ranging from -25% to $+2\%$ (figures 1(d)–(i)). At stations in the typhoon-affected region especially YRD, the simulated wet deposition values of N_{ox} and N_{rd} are very close to their observed counterparts, with NMBs of 4% and 8%, respectively. At stations in the S-high control region, the wet deposition of N_{ox} was overestimated by the model, with an NMB of $+32\%$. Such positive bias in the simulated IN wet deposition is mainly due to the overestimation of N precursors, up to $+20\%$ for NO_x as reported by Ge *et al* (2020).

3. Results

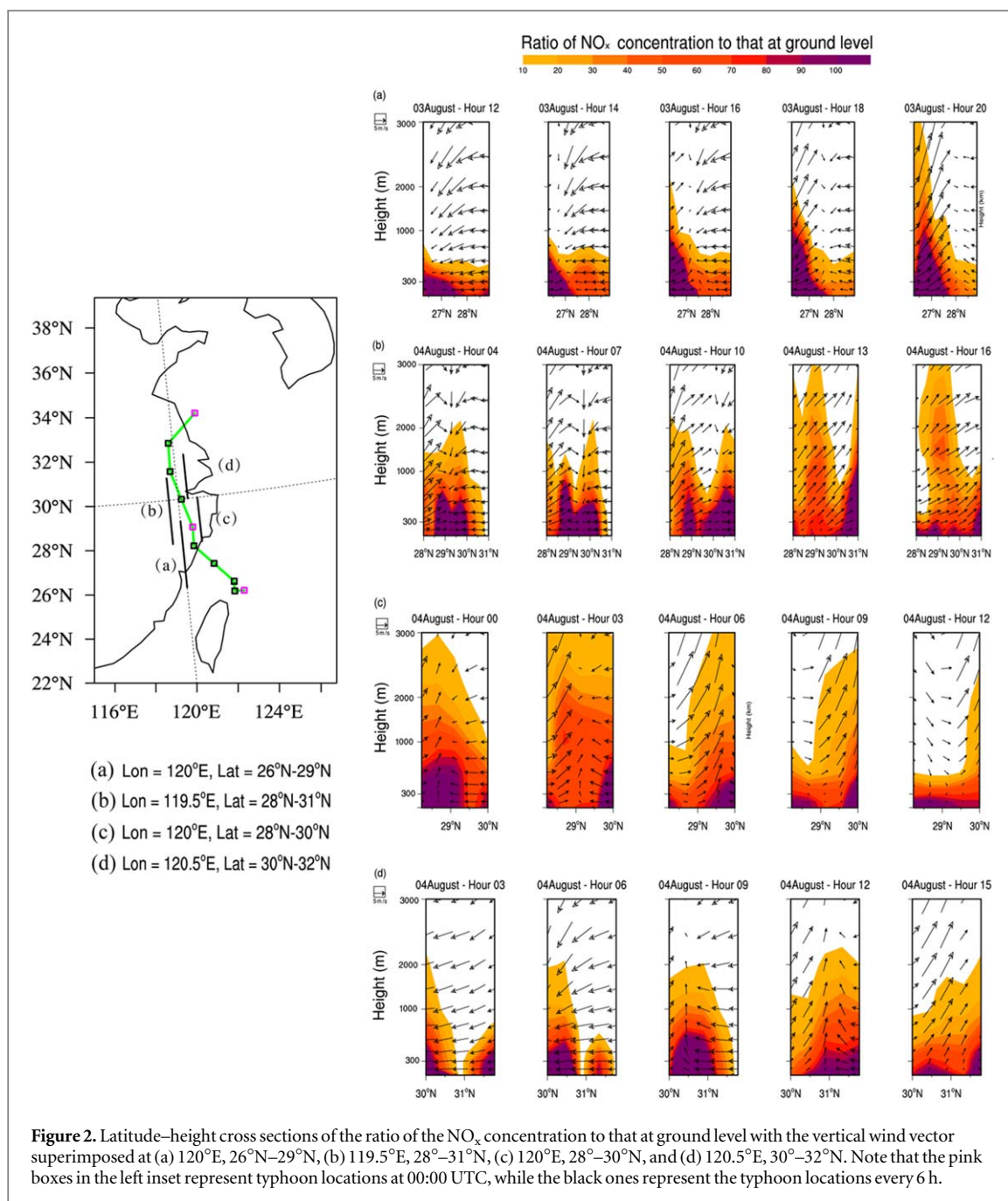
3.1. Typhoon track and typhoon-affected regions

As the track of Hagupit in figure 1(b) (blue lines) shows, the typhoon impacted eastern China after it made landfall in the YRD on 3 August. According to the MODIS true-color image taken on 3 August (figure S3(a)), the location of mostly the cloud-free typhoon eye overlaps with the typhoon position at 00:00 UTC on 3 August. Then, the typhoon continued to move in a northeasterly direction after it entered the Bohai Sea. Finally, it made landfall in SK. The model performance of typhoon track simulation is important to reproduce the structure of typhoon surface precipitation and cloud hydrometeors (Merrill 1984, Irish *et al* 2008, Chavas and Emanuel 2010, Hong *et al* 2020, Kumar *et al* 2020). Besides the well-simulated precipitation by WRF, the typhoon track was also consistent with that obtained from Japan Meteorological Agency (Text S3 and figure S4). The whole typhoon track can be divided into three stages, as figures 1(a)–(c) show, i.e., the pre-landfall stage (1–2 August), the landfall stage (3–4 August), and the post-landfall stage (5–6 August).

3.2. Pumping effect of the typhoon

Figure S5 shows latitude–height cross-sections of the ratio of the $\text{PM}_{2.5}$ concentration to that at ground level with the vertical wind vector superimposed. More than 30%–49% of the $\text{PM}_{2.5}$ concentration at ground level could be lifted to altitudes higher than 2–3 km in less than 10 h. All cross-sections over the landfalling regions of the typhoon simulated by NAQPMS captured these fast and violent uplifts of $\text{PM}_{2.5}$. The gaseous precursor of nitrate and ammonium, NO_x , and NH_3 in the same cross-sections, were also found to be uplifted to high altitudes within a very short time (figures 2 and 3). In particular, NO_x was strongly lifted to as high as about 4 km altitudes (figure 2(c)) due to the strong upward winds in the typhoon, while the lifting of NH_3 was significantly weaker than that of NO_x and $\text{PM}_{2.5}$. This is reasonable that NH_3 is mainly emitted by agricultural sources (e.g., livestock and synthetic fertilizers) located on the surface (Aneja *et al* 2003), whereas NO_x pollution occurs primarily through emissions from the industry at higher altitudes, for example, stack chimney emission (Aneja *et al* 2001). The higher altitude the emission source is, the easier for the pollutants to be uplifted to a higher altitude and hence the more contribution to long-range transport.

Vertical transport of air pollutants can be caused by different mechanisms. Boundary layer turbulent mixing can contribute to the vertical transport of pollutants, but it is limited by the boundary layer height (0.6–0.8 km).

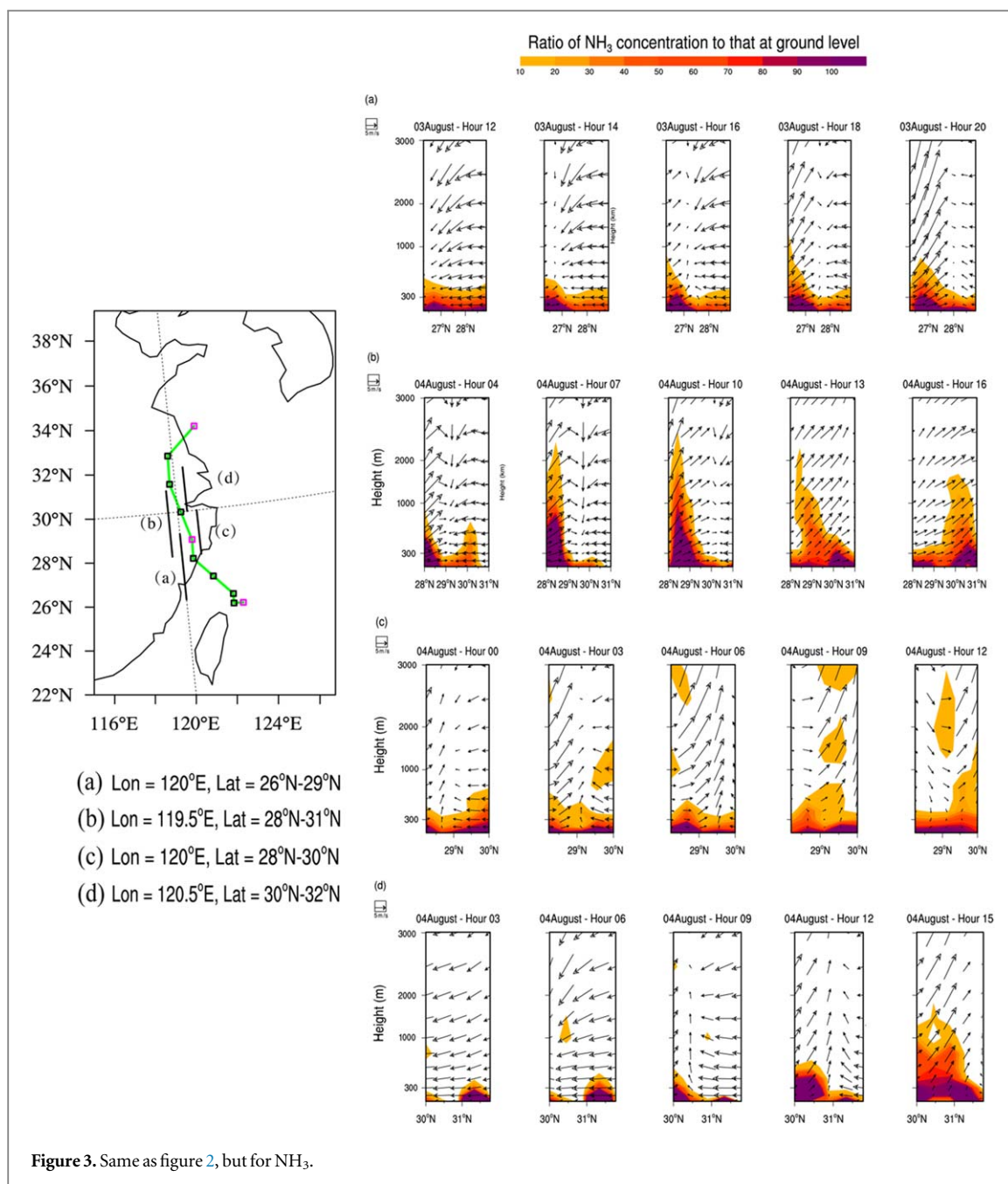


The cold-front structure of most cyclones can also lift pollutants to 1–2.5 km above the ground (Kang *et al* 2019). However, only very strong cyclones such as typhoons may lift air pollutants to almost double the high altitudes that most cyclones can. This indicates that pollutants in the surface layer, such as $\text{PM}_{2.5}$ and NO_x , were quickly lifted to altitudes higher than 2–3 km when typhoon Hagupit made landfall. This elevation of pollutants influenced by the typhoon is hereafter referred to as the typhoon’s ‘pumping effect’ (figure 4).

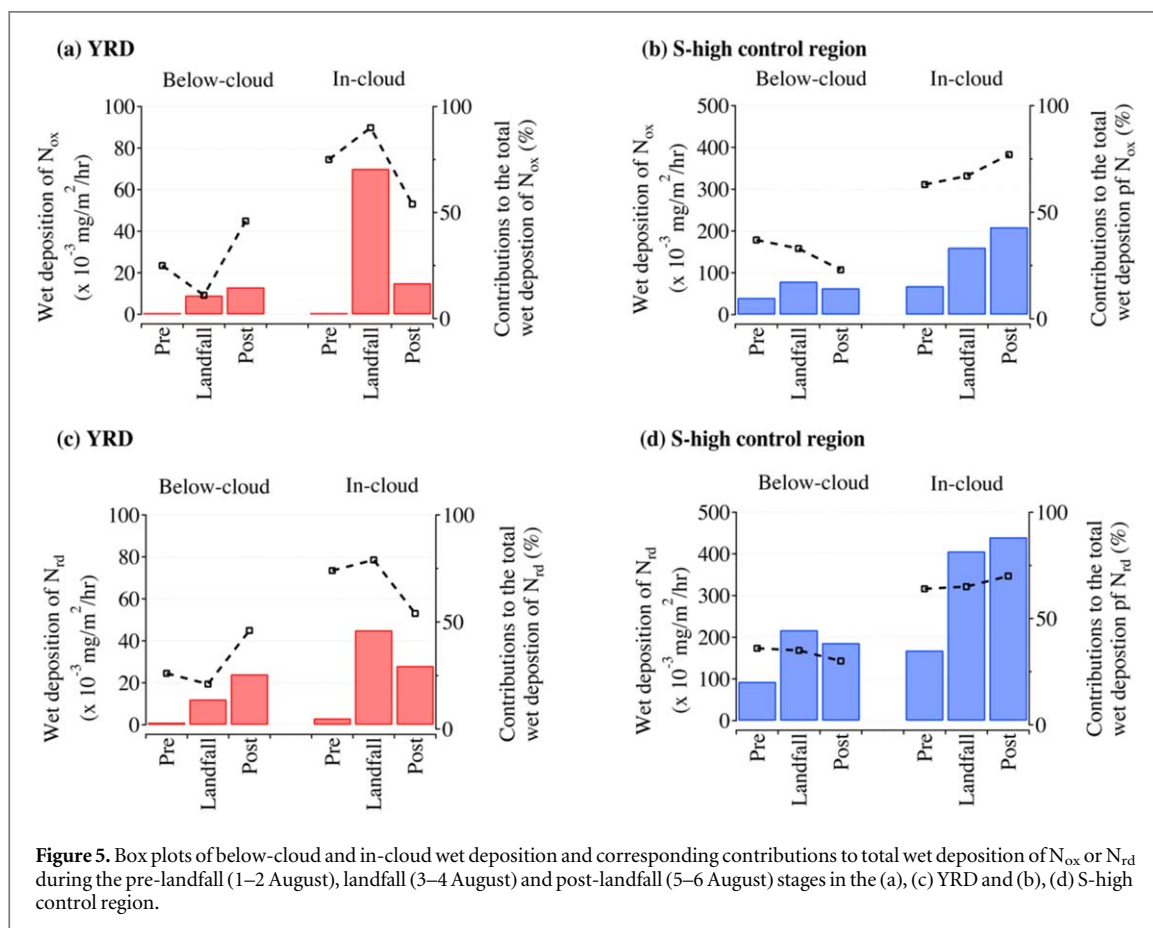
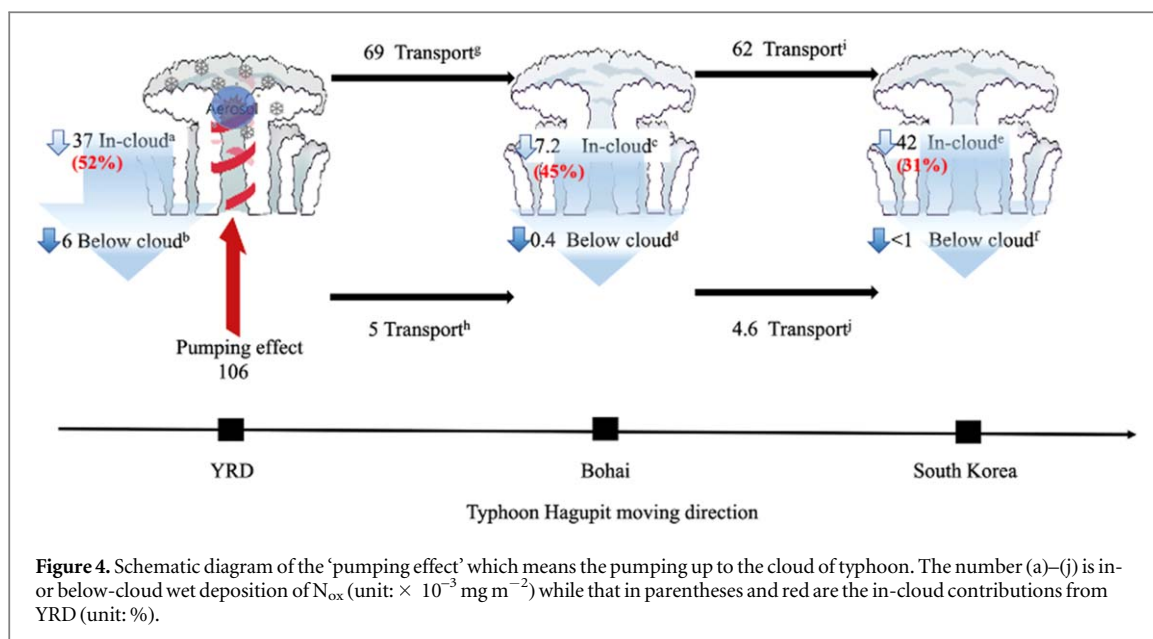
3.3. Contributions from in- and below-cloud scavenging

In order to illustrate the influence of the ‘pumping effect’, wet deposition of IN from in-cloud and below-cloud fractions was recorded by NAQPMs. The typhoon-affected regions in YRD as well as the precipitation region in Shanxi province affected by subtropical anticyclone (hereafter called S-high) are selected to compare the different mechanisms of IN wet deposition. The definition of the S-high region is followed by He *et al* (2015), who use the 5880m geopotential height at 500 hPa to relate with the S-high regions as shown in figure S6, and hence was displayed as the blue rectangle in figure 1.

Box plots of the below- and in-cloud wet deposition and their contributions to the total wet deposition of N_{ox} and N_{rd} during the pre-landfall, landfall, and post-landfall stages in the YRD and S-high region are displayed



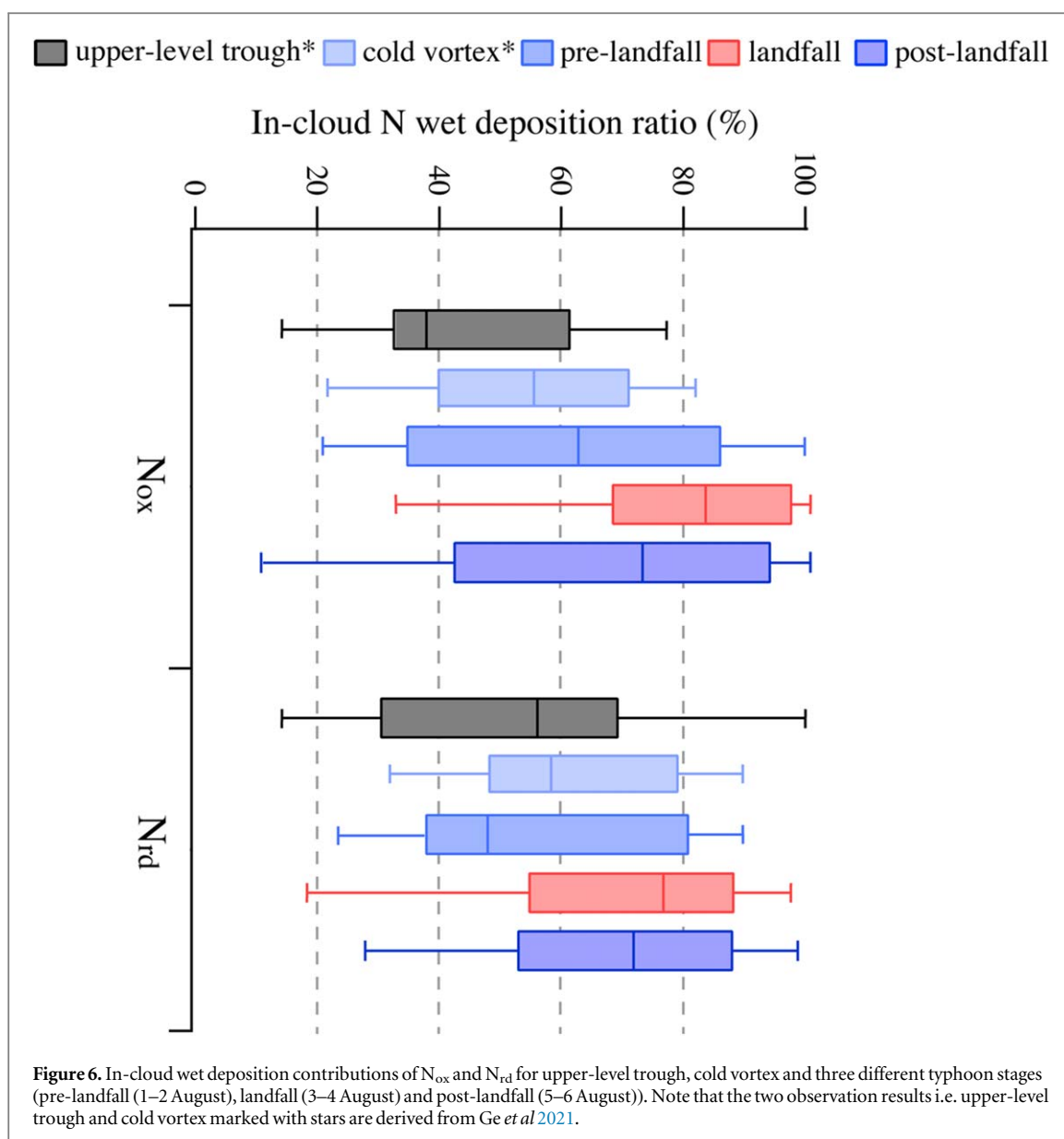
in figure 5. In YRD, with the average precipitation increasing from 5.6 to 21.6 mm, the in-cloud N_{ox} wet deposition contribution changed from 75% during pre-landfall to 89% during landfall. In the S-high region, however, in-cloud N_{ox} wet deposition contribution increased only slightly from 63% to 67%, with the average precipitation increasing from 14 to 27.6 mm. A similar phenomenon is found for N_{rd} wet deposition. Xu *et al* (2017) pointed out that the in-cloud contributions to the total wet deposition will increase with the increase in rainfall as the effect of the washout process weakens. However, the increase of in-cloud contributions is limited by the concentrations of pollutants within the clouds. The larger increase in the typhoon-affected region than in the S-high region indicates the significance of the typhoon's 'pumping effect', which elevates the surface air pollutants to high altitudes and contributes more to the in-cloud scavenging during precipitation events. It is noteworthy that the upper limit of the in-cloud contribution of N_{ox} (N_{rd}) reached 89% (80%) during the typhoon, which is significantly higher than the average value of 39% (53%) in 2014 observed in China (Xu *et al* 2017) and the value of 34% observed in Japan (Aikawa and Hiraki 2009, Aikawa *et al* 2014). The highest value (82%) was found in the cold vortex events during the four years observation in Beijing, China reported by Ge *et al* (2021). This observation confirms that in-cloud contributions for strong convective weather systems like typhoons and cold vortices can be much higher than thought (figure 6, figure S7).



3.4. Source identification into the scavenging pathways

To better characterize the mechanism of nitrogen deposition induced by typhoons, detailed simulations were done using the updated NAQMPS. Different from the previous studies, the source of wet deposition during the typhoon event was firstly identified in relation to wet scavenging processes (figure 7). Three typical typhoon-affected regions, i.e., YRD, Bohai, and SK were chosen as the receptor regions under the influence of typhoon Hagupit to quantitatively investigate the source of in- and below-cloud wet deposition.

For the YRD, the largest source contribution to the in-cloud wet deposition in the YRD was from local emission (table S3), accounting for 52% (38%) of the in-cloud wet deposition of N_{ox} (N_{rd}). The relative



contribution to the below-cloud from YRD was 68% (48%), corresponding up to 8% (9%) of total wet depositions of N_{ox} (N_{rd}). This reveals that local emissions were the dominant source of both in-cloud and below-cloud wet deposition in the YRD. For Bohai, the largest contribution was from emissions in the YRD, reaching up to 47% of the total wet deposition of N_{ox} , which was about four times higher than other sources (table S3). However, pollutants from the YRD contributed significantly less to the in-cloud wet deposition of N_{rd} than that of N_{ox} (1.5 versus $7.2 \times 10^{-3} \text{ mg m}^{-2} \text{ h}^{-1}$, table S3). For SK, the largest in-cloud contributor was also from the YRD. However, the largest contributor to the total wet deposition of N_{ox} in SK was the local emission, which accounted for 32% of the total wet deposition, with 5% from the below-cloud part. Detailed analysis of the S/R relationship in three regions can be found in Text S6 and table S3.

Analysis of IN deposition caused by typhoons in terms of scavenging pathways can shed light on typhoons' effect on the coastal region, optimize the source identification and help to protect the marine ecological environment. This updated S/R relationship of in-cloud wet deposition during the typhoon event challenges the traditional view that the in-cloud wet deposition of acidic pollutants is mainly linked with medium- or long-range transport, which is mainly in non-typhoon events. This significantly higher contribution from the YRD region can be attributed to the 'pumping effect' of the typhoon, which influenced greatly not only the long-range transport of IN from the YRD to Bohai and SK but also the local wet deposition in the YRD itself.

3.5. Implications to the knowledge of IN wet deposition affected by typhoon landfall

What will the mechanism so-called 'pumping effect' of typhoon affect the wet deposition of nitrogen in the downwind typhoon-affected regions. We have quantified the effect of the 'pumping effect' according to the S/R

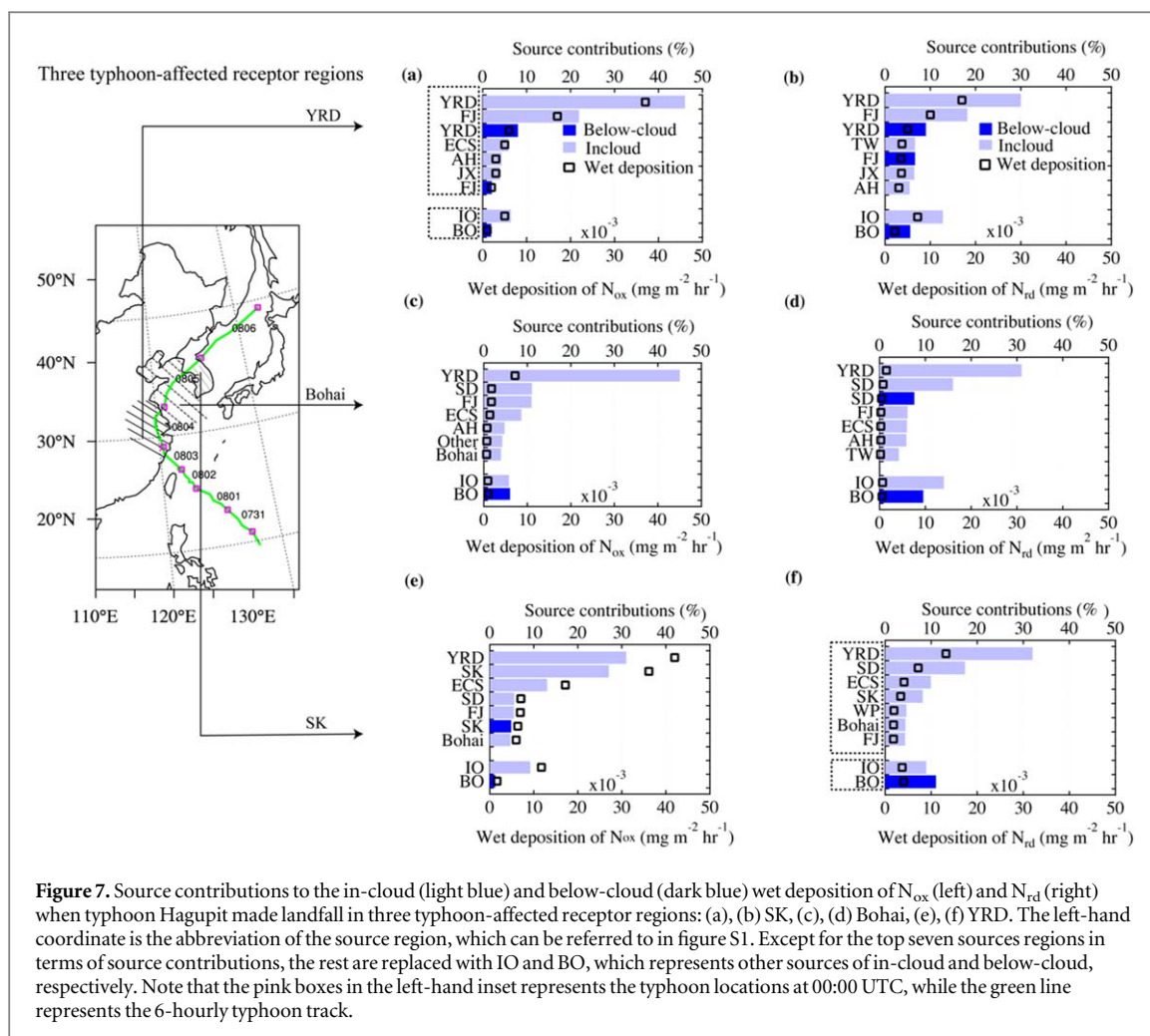


Figure 7. Source contributions to the in-cloud (light blue) and below-cloud (dark blue) wet deposition of N_{ox} (left) and N_{rd} (right) when typhoon Hagupit made landfall in three typhoon-affected receptor regions: (a), (b) SK, (c), (d) Bohai, (e), (f) YRD. The left-hand coordinate is the abbreviation of the source region, which can be referred to in figure S1. Except for the top seven sources regions in terms of source contributions, the rest are replaced with IO and BO, which represents other sources of in-cloud and below-cloud, respectively. Note that the pink boxes in the left-hand inset represents the typhoon locations at 00:00 UTC, while the green line represents the 6-hourly typhoon track.

relationship of N_{ox} wet deposition as figure 4 shows. As section 3.2 described, when typhoon HAGUPIT made landfall in YRD, the $PM_{2.5}$ and NO_x in the multiple cross-sections, were found to be uplifted to higher than 2–3 km in less than 10 h due to deep convective transports associated with cyclones (Fadnavis *et al* 2011). These pollutants were scavenged by the clouds, making the in-cloud wet deposition significant increase in this study.

According to table S3, when typhoon made landfall in YRD, $106 \times 10^{-3} \text{ mg m}^{-2}$ amount of oxidized N were uplifted into the cloud by the pumping effect of typhoon. Meanwhile, with the development of rainfall in YRD, $37 \times 10^{-3} \text{ mg m}^{-2}$ of uplifted N from YRD were scavenged by in-cloud process, which accounts for 52% of the total wet deposition in YRD (a). With the movement of typhoon, the remained amount of $69 \times 10^{-3} \text{ mg m}^{-2}$ oxidized N pollutants (g) induced by pumping effect were transported into downwind typhoon-affected regions such as Bohai and South Korea. This made $7.2 \times 10^{-3} \text{ mg m}^{-2}$ in-cloud wet deposition of N_{ox} (c) in Bohai and $42 \times 10^{-3} \text{ mg m}^{-2}$ in-cloud wet deposition of N_{ox} (e) in South Korea. Different from the in-cloud scavenging, the below-cloud scavenging was much smaller. Almost $6 \times 10^{-3} \text{ mg m}^{-2}$ amounts of oxidized N from local region were washed out and deposited into YRD (b). Due to the airflow supported by typhoon, $5 \times 10^{-3} \text{ mg m}^{-2}$ amounts of oxidized N from YRD (h) were transported below the cloud to downwind areas such as Bohai ($0.4 \times 10^{-3} \text{ mg m}^{-2}$) and South Korea ($<1 \times 10^{-3} \text{ mg m}^{-2}$).

The contributions of long-range transport from the YRD were almost maintained above 40% in Bohai and 30% in SK mainly via the in-cloud process. This means that, as the typhoon moved to downwind areas, the long-range transport of pollutants from the YRD constantly influenced the in-cloud wet deposition in Bohai and SK. The largest source contribution to the in-cloud wet deposition in the YRD was local, which contributed to 52% of the in-cloud wet deposition of N_{ox} . This reveals that local emissions were the dominant source of the in-cloud wet deposition in the YRD. This updated S/R relationship of in-cloud wet deposition during this typhoon event challenges the traditional view that, the in-cloud wet deposition of acidic pollutants is mainly linked with medium- or long-range transport. The above analysis reveals the importance of contributions from emissions in typhoon landing to the typhoon-affected regions. This mechanism of wet deposition due to the ‘pumping effect’ may have profound effects on the wet deposition of N in typhoon-affected areas.

4. Conclusions

The updated wet scavenging module in NAQPMS, coupled with the online tracer tagging method, was used to investigate the sources of in- and below-cloud N wet deposition during the landfall of typhoon Hagupit in the YRD, China. The model was able to capture the observed variations of N_{ox} and N_{rd} during the movement of Hagupit. Based on the NAQPMS simulations as well as the observations, the influence of the so-called ‘pumping effect’ mechanism of the typhoon on the wet deposition of N was explored. This made the air pollutants easy for them to be captured by cloud droplets and deposited via the in-cloud scavenging process, which contributed to 80%–89% of the wet deposition of N in the typhoon-affected region. In addition, the present study has improved our knowledge of the S/R relationship of the wet deposition of N during the landfall stage of typhoons in China, especially the in- and below-cloud processes of wet deposition. As the landfall region for Hagupit, the YRD was found to be the largest contributor of wet deposition via the in-cloud process, not only for itself but also in the other regions of Hagupit’s pathway, i.e., the Bohai Sea and South Korea. This can be attributed to the ‘pumping effect’, which contributes to a large proportion of the in-cloud wet deposition in the downwind typhoon-affected regions. Continuous observations of wind profile radar combined with aircraft data show that the vertical wind profile and intensity of pressure are of crucial importance for determining a tropical cyclone’s radial inflow (Liao *et al* 2019). This means that the amounts of pollutants which typhoon pumps into are closely related to model simulation of the intensity of the typhoon itself. The simulation of intensity pressure of typhoon, especially the central pressure does not reach the actual observation. The error caused by the typhoon simulation of air pressure could affect the model performance on pumping volume. Fujita *et al* (2004) observed the inflow height would get stronger as typhoon moved to north-eastward. Probably, with typhoon moving north-eastward the height of ‘pumping effect’ can reach beyond the 2–3 km, which was found in this study, and this uncertainty will further lead to uncertainty in the amount of in-cloud scavenging, long-range transport and the deposition. Besides, improving the model performance of the central pressure of typhoon should also be considered in future. Also, different typhoons would have multiple and variable height of ‘pumping effect’, which should be examined with typhoon moving north-east.

Acknowledgments

This work was financially supported by the National Science Foundation of China (Grants 42122049), and the National Key R&D Program of China (2022YFC3702002) and the Strategic Priority Research Program (A) of the Chinese Academy of Sciences (Grant XDA19040204).

Data availability statement

All data that support the findings of this study are included within the article (and any supplementary files).

ORCID iDs

Qixin Tan  <https://orcid.org/0000-0002-2034-472X>

Syuichi Itahashi  <https://orcid.org/0000-0001-7567-7831>

Joshua S Fu  <https://orcid.org/0000-0001-5464-9225>

References

- Aikawa M and Hiraki T 2009 Washout/rainout contribution in wet deposition estimated by 0.5 mm precipitation sampling/analysis *Atmos. Environ.* **43** 4935–39
- Aikawa M, Kajino M, Hiraki T and Mukai H 2014 The contribution of site to washout and rainout: Precipitation chemistry based on sample analysis from 0.5 mm precipitation increments and numerical simulation *Atmos. Environ.* **95** 165–74
- Aneja V P *et al* 2001 Atmospheric nitrogen compounds II: emissions, transport, transformation, deposition and assessment *Atmos. Environ.* **35** 1903–11
- Aneja V P, Nelson D R, Roelle P A, Walker J T and Battye W 2003 Agricultural ammonia emissions and ammonium concentrations associated with aerosols and precipitation in the southeast United States *J. Geophysical Research-Atmospheres* **108** 4152
- Bender M A, Knutson T R, Tuleya R E, Sirutis J J, Vecchi G A, Garner S T and Held I M 2010 Modeled impact of anthropogenic warming on the frequency of intense Atlantic hurricanes *Science* **327** 454–58
- Chavas D R and Emanuel K A 2010 A quikscat climatology of tropical cyclone size *Geophys. Res. Lett.* **37**
- Chen X *et al* 2017 Estimation of atmospheric aging time of black carbon particles in the polluted atmosphere over central-eastern China using microphysical process analysis in regional chemical transport model *Atmos. Environ.* **163** 44–56
- Chen Y X *et al* 2015 Dissolved organic nitrogen in wet deposition in a coastal city (Keelung) of the southern East China Sea: Origin, molecular composition and flux *Atmos. Environ.* **112** 20–31

- Chiang P C, Chang E E, Chang T C and Chiang H L 2005 Seasonal source-receptor relationships in a petrochemical industrial district over northern Taiwan *J. Air Waste Manag Assoc* **55** 326–41
- Dennis R L, McHenry J N, Barchet W R, Binkowski F S and Byun D W 1993 Correcting RADM's sulfate underprediction: Discovery and correction of model errors and testing the corrections through comparisons against field data *Atmos. Environ. Part A* **27** 975–97
- Doney S C, Mahowald N, Lima I, Feely R A, Mackenzie F T, Lamarque J F and Rasch P J 2007 Impact of anthropogenic atmospheric nitrogen and sulfur deposition on ocean acidification and the inorganic carbon system *Proc Natl Acad Sci U S A* **104** 14580–85
- Du E 2018 A database of annual atmospheric acid and nutrient deposition to China's forests *Sci. Data* **5** 180223
- Du H Y *et al* 2019 Modeling of aerosol property evolution during winter haze episodes over a megacity cluster in northern China: roles of regional transport and heterogeneous reactions of SO₂ *Atmos. Chem. Phys.* **19** 9351–70
- Fadnavis S, Beig G, Buchunde P, Ghude S D and Krishnamurti T N 2011 Vertical transport of ozone and CO during super cyclones in the Bay of Bengal as detected by Tropospheric Emission Spectrometer *Environ. Sci. Pollut. Res. Int.* **18** 301–15
- Fang G C, Lin S J, Chang S Y and Chou C C K 2009 Effect of typhoon on atmospheric particulates in autumn in central Taiwan *Atmos. Environ.* **43** 6039–48
- Fujita H, Teshiba M, Umemoto Y, Shibagaki Y, Hashiguchi H, Yamanaka M and Fukao S 2004 Study on the extratropical transition of typhoon 0310 (Etau) observed by wind profilers and weather radars *Proc. of ERAD*
- Ge B *et al* 2020 Model Inter-Comparison Study for Asia (MICS-Asia) phase III: multimodel comparison of reactive nitrogen deposition over China *Atmos. Chem. Phys.* **20** 10587–610
- Ge B Z *et al* 2021 Inter-annual variations of wet deposition in Beijing from 2014–2017: implications of below-cloud scavenging of inorganic aerosols *Atmos. Chem. Phys.* **21** 9441–54
- Ge B Z, Wang Z F, Xu X B, Wu J B, Yu X L and Li J 2014 Wet deposition of acidifying substances in different regions of China and the rest of East Asia: modeling with updated NAQPMS *Environ. Pollut.* **187** 10–21
- Grewe V 2004 Technical Note: A diagnostic for ozone contributions of various NO_x emissions in multi-decadal chemistry-climate model simulations *Atmos. Chem. Phys.* **4** 729–736
- Hao Y J, Tang D L, Yu L and Xing Q G 2011 Nutrient and chlorophyll a anomaly in red-tide periods of 2003–2008 in Sishili Bay, China *Chin. J. Oceanol. Limnol.* **29** 664–73
- He C, Zhou T, Lin A, Wu B, Gu D, Li C and Zheng B 2015 Enhanced or weakened western north pacific subtropical high under global warming? *Sci. Rep.* **5** 16771
- Holloway T, Levy H and Carmichael G 2002 Transfer of reactive nitrogen in Asia: development and evaluation of a source-receptor model *Atmos. Environ.* **36** 4251–64
- Hong W, Zheng Y L, Chen B, Su T H and Ke X Q 2020 Monthly variation and spatial distribution of quadrant tropical cyclone size in the Western North Pacific *Atmos. Sci. Lett.* **21** e956
- Irish J L, Resio D T and Ratcliff J J 2008 The influence of storm size on hurricane surge *J. Phys. Oceanogr.* **38** 2003–13
- Itahashi S *et al* 2020 MICS-Asia III: overview of model intercomparison and evaluation of acid deposition over Asia *Atmos. Chem. Phys.* **20** 2667–93
- Kajino M, Sato K, Inomata Y and Ueda H 2013 Source-receptor relationships of nitrate in Northeast Asia and influence of sea salt on the long-range transport of nitrate *Atmos. Environ.* **79** 67–78
- Kajino M, Ueda H, Sato K and Sakurai T 2011 Spatial distribution of the source-receptor relationship of sulfur in Northeast Asia *Atmos. Chem. Phys.* **11** 6475–91
- Kang H Q *et al* 2019 Potential impacts of cold frontal passage on air quality over the Yangtze River Delta, China *Atmos. Chem. Phys.* **19** 3673–85
- Knotkova D and Barton K 1992 Effects of acid deposition on corrosion of metals *Atmospheric Environment. Part a-General Topics* **26** 3169–77
- Knutson T, Landsea C and Emanuel K 2010 Tropical cyclones and climate change: a review *In Global Perspectives on Tropical Cyclones* **4** 243–84
- Kong L *et al* 2020 Evaluation and uncertainty investigation of the NO₂, CO and NH₃ modeling over China under the framework of MICS-Asia III *Atmos. Chem. Phys.* **20** 181–202
- Kumar S, Panda J, Singh K, Guha B K and Kant S 2020 Structural characteristics of North Indian Ocean tropical cyclones during 1999–2017: a scatterometer observation-based analysis *Theor. Appl. Climatol.* **143** 227–40
- Li J *et al* 2008 Near-ground ozone source attributions and outflow in central eastern China during MTX2006 *Atmos. Chem. Phys.* **8** 7335–51
- Li J *et al* 2011 Impacts of aerosols on summertime tropospheric photolysis frequencies and photochemistry over Central Eastern China *Atmos. Environ.* **45**
- Li J *et al* 2013 Assessing the effects of trans-boundary aerosol transport between various city clusters on regional haze episodes in spring over East China *Tellus B: Chemical and Physical Meteorology* **65** 20052
- Li J *et al* 2016 Modeling study of surface ozone source-receptor relationships in East Asia *Atmos. Res.* **167**
- Li J *et al* 2019 Model evaluation and intercomparison of surface-level ozone and relevant species in East Asia in the context of MICS-Asia Phase III—Part 1: Overview *Atmos. Chem. Phys.* **19** 12993–13015
- Li M *et al* 2017 MIX: a mosaic asian anthropogenic emission inventory under the international collaboration framework of the MICS-Asia and HTAP *Atmos. Chem. Phys.* **17** 935–63
- Liao F, Su R, Chan P-W, Qi Y and Hon K-K 2019 Observational study on the characteristics of the boundary layer during changes in the intensity of tropical cyclones landing in guangdong, China *Advances in Meteorology* **2019** 8072914
- Lin M, Oki T, Bengtsson M, Kanae S, Holloway T and Streets D G 2008 Long-range transport of acidifying substances in east Asia - Part II - Source-receptor relationships *Atmos. Environ.* **42** 5956–67
- Lin T C, Hamburg S P, King H B and Hsia Y J 2000 Throughfall patterns in a subtropical rain forest of northeastern Taiwan *J. Environ. Qual.* **29** 1186–93
- Merrill R T 1984 A comparison of large and small tropical cyclones *Mon. Weather Rev.* **112** 1408–18
- Okin G S *et al* 2011 Impacts of atmospheric nutrient deposition on marine productivity: Roles of nitrogen, phosphorus, and iron *Global Biogeochem. Cycles* **25**
- Page T, Whyatt J D, Metcalfe S E, Derwent R G and Curtis C 2008 Assessment of uncertainties in a long range atmospheric transport model: Methodology, application and implications in a UK context *Environ. Pollut.* **156** 997–1006
- Pitcairn C E, Fowler D, Leith I D, Sheppard L J, Sutton M A, Kennedy V and Okello E 2003 Bioindicators of enhanced nitrogen deposition *Environ. Pollut.* **126** 353–61
- Sakihama H and Tokuyama A 2005 Effect of typhoon on chemical composition of rainwater in Okinawa Island, Japan *Atmos. Environ.* **39** 2879–88

- Santachiara G, Prodi F and Belosi F 2012 A review of termo- and diffusio-phoresis in the atmospheric aerosol scavenging process. Part 1: drop scavenging *Atmospheric and Climate Sciences* **02** 148–58
- Seinfeld J H and Pandis S N 2016 *Atmospheric Chemistry and Physics: From air Pollution to Climate Change*. **20** 953–964
- Skamarock W *et al* 2008 *A Description of the Advanced Research WRF Version 3*
- Tan J N *et al* 2018 Multi-model study of HTAP II on sulfur and nitrogen deposition *Atmos. Chem. Phys.* **18** 6847–66
- Tian Y *et al* 2020 Influence of the morphological change in natural Asian dust during transport: A modeling study for a typical dust event over northern China *Sci. Total Environ.* **739** 139791
- Toyonaga S and Zhang D 2016 Wet deposition fluxes of ions contributed by cyclone-, stationary front- and typhoon-associated rains at the Southwestern Japan Coast *Asian J. Atmospheric Environment* **10** 57–66
- Wang J, Yu Z, Wei Q and Yao Q 2019 Long-term nutrient variations in the bohai sea over the past 40 years *J. Geophysical Research: Oceans* **124** 703–22
- Wang Z *et al* 2017 Modeling the long-range transport of particulate matters for january in East Asia using NAQPMS and CMAQ *Aerosol Air Qual. Res.* **17** 3065–78
- Wang Z F, Maeda T, Hayashi M, Hsiao L F and Liu K Y 2001 A nested air quality prediction modeling system for urban and regional scales: Application for high-ozone episode in Taiwan *Water Air Soil Pollut.* **130** 391–96
- Webster P J, Curry J A, Liu J and Holland G J 2006 Response to comment on ‘Changes in tropical cyclone number, duration, and intensity in a warming environment’ *Sci.* **311** 1713
- Wu J B *et al* 2017 Development of an on-line source-tagged model for sulfate, nitrate and ammonium: A modeling study for highly polluted periods in Shanghai, China *Environ. Pollut.* **221** 168–79
- Xu D *et al* 2017 Below-cloud wet scavenging of soluble inorganic ions by rain in Beijing during the summer of 2014 *Environ. Pollut.* **230** 963–73
- Xu D H *et al* 2019 Multi-method determination of the below-cloud wet scavenging coefficients of aerosols in Beijing, China *Atmos. Chem. Phys.* **19** 15569–81
- Yan J, Chen L, Lin Q, Zhao S and Zhang M 2016 Effect of typhoon on atmospheric aerosol particle pollutants accumulation over Xiamen, China *Chemosphere* **159** 244–55
- Yang W, Li J, Wang M, Sun Y and Wang Z 2018 A Case Study of Investigating Secondary Organic Aerosol Formation Pathways in Beijing using an Observation-based SOA Box Model *Aerosol Air Qual. Res.* **18** 1606–16
- Zhang J, Zhang Z F, Liu S M, Wu Y, Xiong H and Chen H T 1999 Human impacts on the large world rivers: Would the Changjiang (Yangtze River) be an illustration? *Global Biogeochem. Cycles* **13** 1099–1105